. International Journal on Recent and Innovation Trends in Computing and Communication ISSN: 2321-8169
Volume: 5 Issue: 3 422 – 427

Six Step Control vs Direct Torque Control comparative evaluation for BLDC drive

Hassan Hadeed and Achim Gottscheber

***Abstract*—This research paper deals with the two closed loop speed control algorithms namely Six-Step and Direct Torque Control for Brushless DC Motor Drive. These two control techniques are critically evaluated for the performance comparison in terms of efficiency, steady state response and transient condition. The simulation models of the two controllers are developed in MATLAB/SIMULINK environment. The simulation results show close agreements and provide good insight for the evaluation of these two control techniques.**

***Index Terms*—Six Step Control, Direct Torque Control, Brushless DC Motor, Space Vector Modulation.**

I. Introduction

THE recent and future generation of electric motors mainly depend on the speed driving systems which have high efficiency, robust, smaller size and less noisy drive, however, for such requirement BLDC motors are very much advisable. Also, the research is more focusing on BLDC motors drive. BLDC motor is a type of synchronous motor which does not operate using brushes, rather it operates with a controller via electronic commutation in which it is characterized by its unique trapezoidal back electromotive force waveform. Speed ripples occur due to the power electronic commutation, imperfections in the stator , Furthermore, the non-linearity in the commutation schema [1], however an effective controller is required to minimize the ripples and improve the performance of the drive.

In [2], present a DTC of BLDC motor fed by four-switch inverters rather than six-switch inverters in conventional drives. In [3], DTC has proposed to minimize torque ripple of BLDC motors with un-ideal back electromotive force (EMF) waveforms. In [4], An improved direct torque control of brushless DC motors using twelve voltage space vectors has been implemented rather than six space vectors. In [5], an optimal current excitation scheme was proposed based on pre-optimized waveforms in the dq axes transformation for reference current which results in minimum torque ripple and copper losses. In [6], an effective method with instantaneous torque control was proposed with reduce torque ripple, but it was only applicable to two-phase BLDC operating in the 120 conduction mode, and not to the 180 conduction mode.

Hassan Hadeed is currently pursuing master of engineering in information technology at SRH University Heidelberg, Germany (e-mail: san.hadeed@gmail.com)

Dr. Achim Gottscheber is a Professor and Head of Electrical Engineering and Information Technology at SRH University Heidelberg, Germany (e-mail: achim.gottscheber@fh-heidelberg.de)

This paper present the implementation of six-step and direct torque control algorithms to control the three-phase trapezoidal brushless DC motor with concentrated stator windings fed by six-switch inverter (MOSFET) to achieve the required result, therefore, Simulation results will demonstrate the essential differences between the DTC and 6-step for BLDC drive.

A. Six-Step for BLDC Motor Drive

It based on using 6 distinct steps according to an angle of 60° electrical rotation angle. The name trapezoidal refers to the current waveform and the back electromotive force shape which is produced by this method. However, the 6-step algorithm is based on sensing the rotor position by using a three hall sensors which embedded into the motor drive. These hall sensors are placed every 120°, with these sensors, six different commutations are possible, moreover, phase commutation depends on hall sensor values. Fig. 1, shows the schematic of 6-Step method.

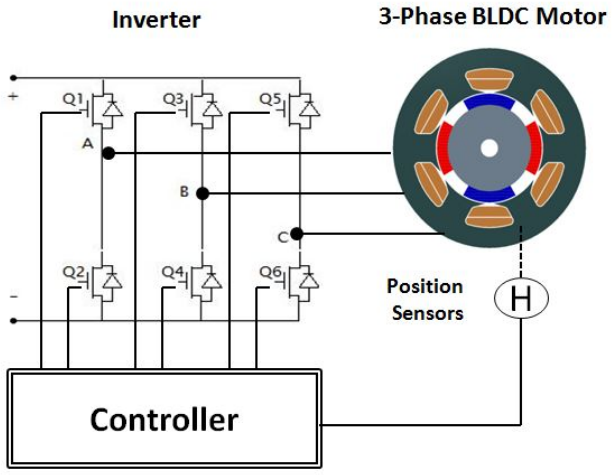

Fig. 1. Schematic of Six-Step Commutation

B. DTC for BLDC Motor Drive

DTC is a method used to control the variable frequency drives which leads to control the torque of the motor. This involves the estimation of both the magnetic flux and torque based on the measured voltage and current of the motor and compare them to reference value, as a result error signal will

generate and directly controls the six switch inverter to keep the torque and flux within the limits of the hysteresis band. Fig. 2, illustrates the DTC for BLDC drive.

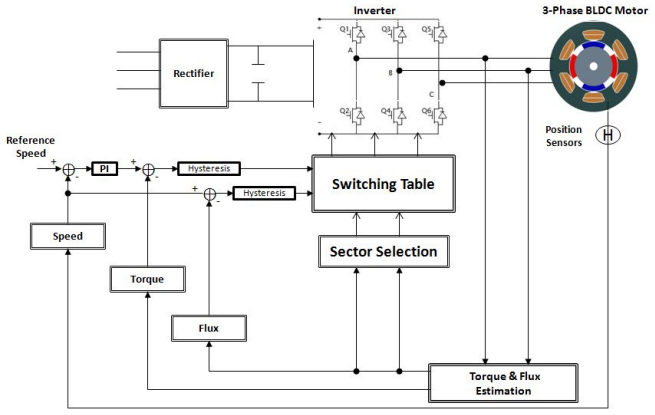

Fig. 2. Schematic of DTC for BLDC drive

The electromagnetic torque of a permanent-magnet brushless machine in the synchronously rotating dq rotating reference frame can be calculated as [6,7]

$$T_e = \frac{3}{2}\frac{p}{2}[(\frac{dL_d}{d\theta_e}i_{sd} + \frac{d\Psi_{rd}}{d\theta_e} - \Psi_{sq})i_{sd} + (\frac{dL_q}{d\theta_e}i_{sq} + \frac{d\Psi_{rq}}{d\theta_e} + \Psi_{sd})i_{sq}] \quad (1)$$

where

$$\Psi_{sq} = L_q i_{sq} + \Psi_{rq} \quad (2)$$

$$\Psi_{sd} = L_d i_{sd} + \Psi_{rd} \quad (3)$$

and p number of poles, i_{sd} and i_{sq} are the d and q-axes currents, θ_r represent the rotor angle, L_d and L_q are the d and q inductances, respectively, and Ψ_{rd}, Ψ_{rq}, Ψ_{sd}, and Ψ_{sq} are the d and q of rotor and stator flux linkages, respectively. For concentrated stator windings with trapezoidal waveform brushless DC drive, the electromagnetic torque for BLDC motor operation, can be simplified in the stationary $\alpha\beta$ reference frame as

$$T_e = \frac{3}{2}\frac{p}{2}[(\frac{d\Psi_{r\alpha}}{d\theta_e}i_{s\alpha} + \frac{d\Psi_{r\beta}}{d\theta_e}i_{s\beta}] \quad (4)$$

where $\Psi_{r\alpha}$ and $\Psi_{r\beta}$ are the α and β axes rotor flux linkages, respectively, and

$$\Psi_{r\alpha} = \Psi_{rd}\cos\theta_e - \Psi_{rq}\sin\theta_e \quad (5)$$

$$\Psi_{r\beta} = \Psi_{rd}\sin\theta_e + \Psi_{rq}\cos\theta_e \quad (6)$$

the stator flux-linkage vectors can be estimated from the measured of stator currents $i_{s\alpha}$ and $i_{s\beta}$ and voltages $u_{s\alpha}$ and $u_{s\beta}$ as [6]

$$\Psi s\alpha = \int (u_{s\alpha} - Ri_{s\alpha})dt \quad (7)$$

$$\Psi s\beta = \int (u_{s\beta} - Ri_{s\beta})dt \quad (8)$$

where R is the stator resistance. The angular position θ of the stator flux linkage vector is obtained as

$$\theta = arctan\frac{\Psi s\beta}{\Psi s\alpha} \quad (9)$$

the rotor flux can be obtained from the stator flux in the $\alpha\beta$ stationary frame as

$$\Psi r\alpha = \Psi s\alpha - Ls^i s\alpha \quad (10)$$

$$\Psi r\beta = \Psi s\beta - Ls^i s\beta \quad (11)$$

The inverter switching pulses are represent in six binary variables and the binary (1) represents the state ON, while the binary (0) represent the state OFF, which are the active voltage vectors [6,8]. Fig. 3, shows the six active voltage vectors of the inverter.

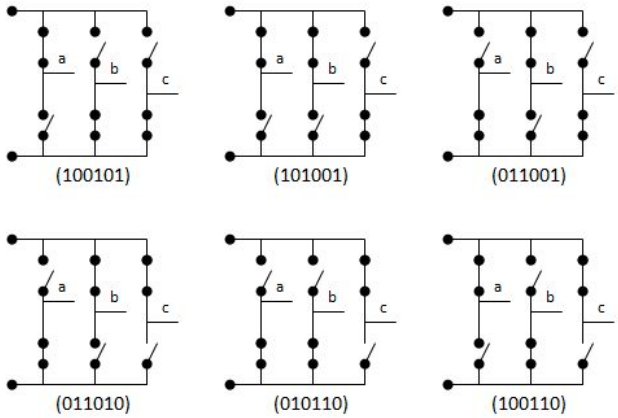

Fig. 3. Switching Sequence of the Inverter with DTC

The corresponding switching combination of the inverter can represent in 6 binary digits, one digit for each leg. Therefore, the active voltage vectors V1,V2,V3,V4,V5 and V6 are define as switching signals (100101), (101001), (011001), (011010), (010110), (100110), respectively, where, from left right, the binary values denote the states of the upper and lower inverter switching sequence for phases A, B and C , respectively [6], and the two non-active null voltage vector V0 and V7 can identify as (010101) and (101010), respectively. Table I below shows the switching table for BLDC motor.

The zone in which the three phase stator axes of the motor is splitted into 6 active voltage space vectors which enable the voltage vector to be selected in terms of the stator flux-linkage vector and each sector can be composed of two active voltage space vectors and two non-active voltage vectors [8], as shown in Fig. 4

ISSN: 2321-8169
422 – 427

Flux Φ	Torque T	Sector					
		1	2	3	4	5	6
1	1	V2 (101001)	V3 (011001)	V4 (011010)	V5 (010110)	V6 (100110)	V1 (100101)
	0	**V0 (010101)**	**V7 (101010)**	**V0 (010101)**	**V7 (101010)**	**V0 (010101)**	**V7 (101010)**
	-1	V6 (100110)	V1 (100101)	V2 (101001)	V3 (011001)	V4 (011010)	V5 (010110)
0	1	V3 (011001)	V4 (011010)	V5 (010110)	V6 (100110)	V1 (100101)	V2 (101001)
	0	**V7 (101010)**	**V0 (010101)**	**V7 (101010)**	**V0 (010101)**	**V7 (101010)**	**V0 (010101)**
	-1	V5 (010110)	V6 (100110)	V1 (100101)	V2 (101001)	V3 (011001)	V4 (011010)

TABLE I
SWITCHING TABLE FOR DTC OF BLDC DRIVER

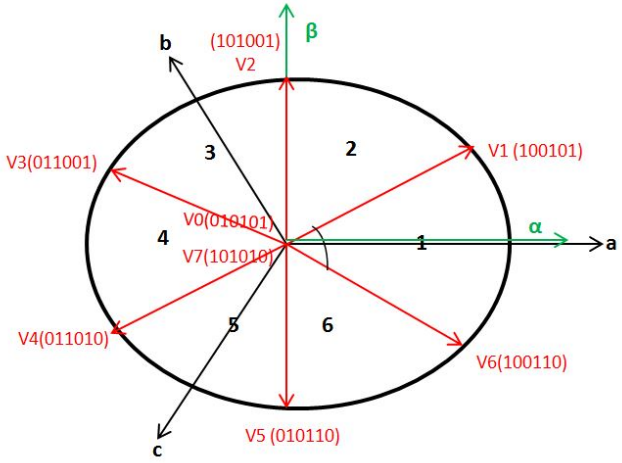

Fig. 4. Sectors Selection for BLDC Drive with DTC

C. Simulation Model of Six-Step Algorithm

Fig. 5, represents the model and the design of six-step schema in simulink. Sensing the output of the BLDC motor will feed back and compare to reference speed, however, that will generate error signal, hence this error signal will processed into PI controller and will generate corresponding output, based on that corresponding output the six-pulse inverter will generate the pulses which control the speed of the BLDC drive. To control the gate pulse of the inverter, rotor positions of BLDC motor have to be sent by using hall effect sensors as per pre-designed true table. It will generate the control signal and based of that signal it will provide switching button, in result, will decide which switch has to be on and what time, therefore control the motor.

MATLAB / Simulink R2016b software is used to perform the simulation for both algorithms, the motor parameters are real-time and has been taken from the data sheet of commercially available BLDC motor as shown in Table II. Running the simulation for $t = 0.03s$ and applying a load

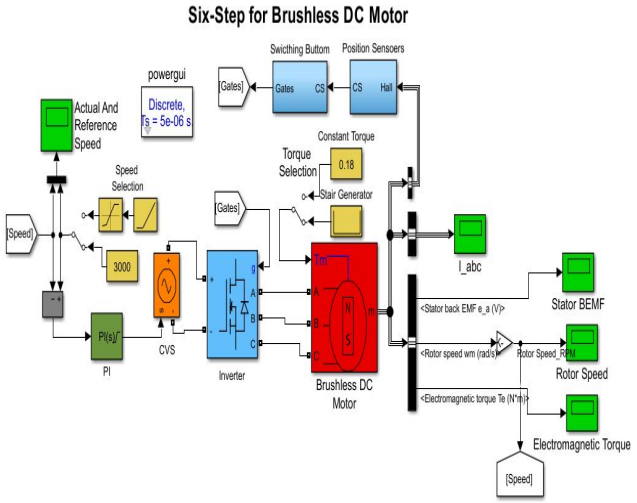

Fig. 5. Simulink Model of 6-Step Algorithm for BLDC Motor Drive with DTC

torque of $0.18Nm$ to the motor shaft at $t = 0.01s$ of the simulation time and removed at $t = 0.02s$.

The electromagnetic varies in accordance with the load torque, however, sawtooth shape observed will cause noisy motor during the operation, also the Back-EMF varies in accordance with the load torque as shown in Fig. 6 and Fig. 7, respectively,

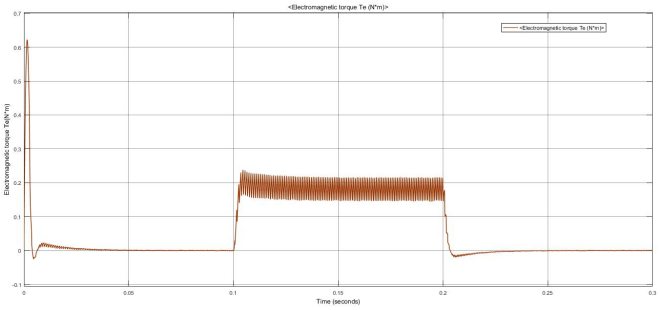

Fig. 6. Time vs Electromagnetic torque under load condition with 6-Step

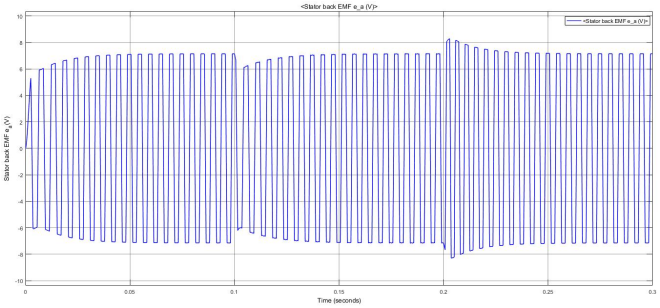

Fig. 7. Time vs Back-EMF under load condition with 6-Step

The initial current at starting point is high and decreases during the acceleration of the motor to reach the nominal speed, however, observe the sawtooth waveform of the 3-phase current, occurred by the DC bus voltage which applies a constant during $120°$ to the motor inductances, furthermore, the stator current increases at the point we applied torque to maintain the nominal speed but remain within the limitation and as per the date sheet of the motor as showing in Fig. 8.

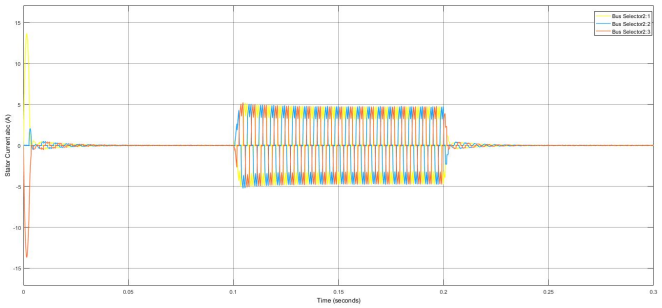

Fig. 8. Time vs Stator Current under load condition with 6-Step

A fluctuation in speed at point we applied force, also the actual speed will take a while to go back and follow the reference speed, furthermore, a huge undershooting and overshooting at point we applied and removed force, respectively, as showing in Fig. 9 and zooming Fig. 10, respectively.

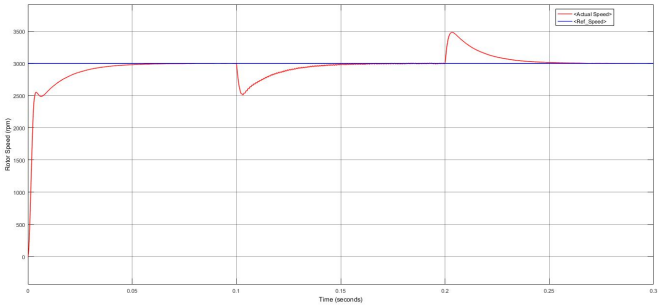

Fig. 9. Time vs Speed under load condition with 6-Step

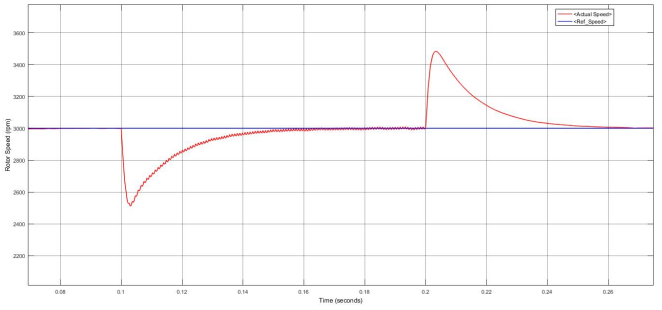

Fig. 10. Time vs Zooming Speed under load condition with 6-Step

D. Simulation of DTC Algorithm

Fig. 11, presents the model and the design of direct torque control schema in simulink. Measuring the stator phase currents and voltages and employing $\alpha\beta$ stationary reference frame transformation, the stator flux linkage vectors and electromagnetic torque can be obtained as showing in Fig. 12.

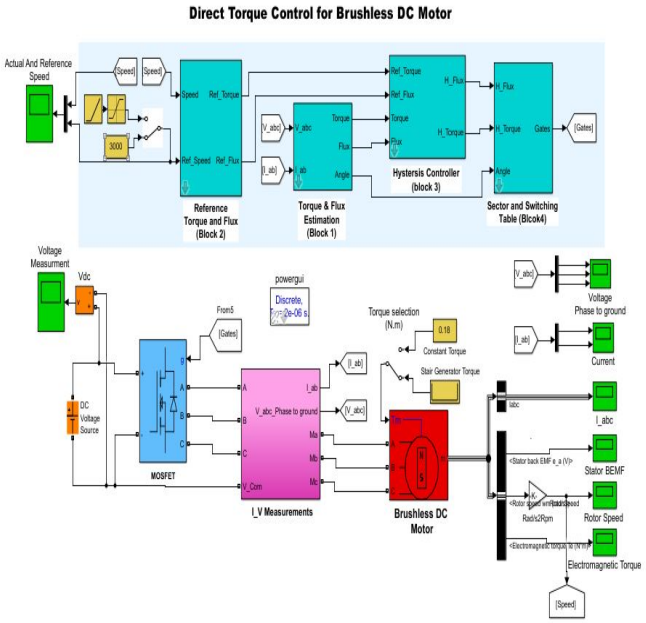

Fig. 11. Simulink Model of DTC Algorithm for the BLDC Motor

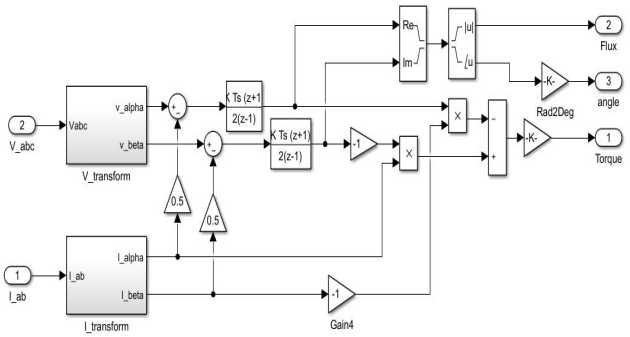

Fig. 12. Sub-block of Torque and Flux estimation with DTC

From the rotor position sensors of the motor we derived the speed feedback and compared it to the reference speed to form the reference torque through proportional integral (PI) speed regulator and also the reference flux. By comparing the estimated electromagnetic torque and stator flux linkage with their reference value through hysteresis controllers, the stator flux-linkage and torque commands are obtained as shown in Fig. 13,

ISSN: 2321-8169
422 – 427

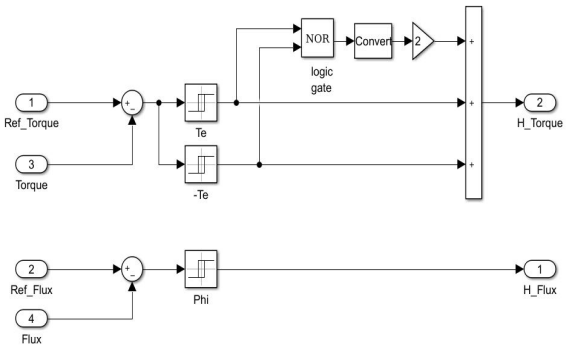

Fig. 13. Sub-block of Torque and Flux Hysteresis with DTC

The switching pattern of the inverter can be determined based on the stator flux-linkage status, torque status and the sector in which the stator flux linkage is located at that instant of time as shown in Fig. 14, thus, voltage source inverter is then controlled by the space vector modulation method in order to output the desired reference voltage, however, using these values the inverter gives the required input voltage to the BLDC motor, and finally the dynamic response of the drive and torque control is achieved.

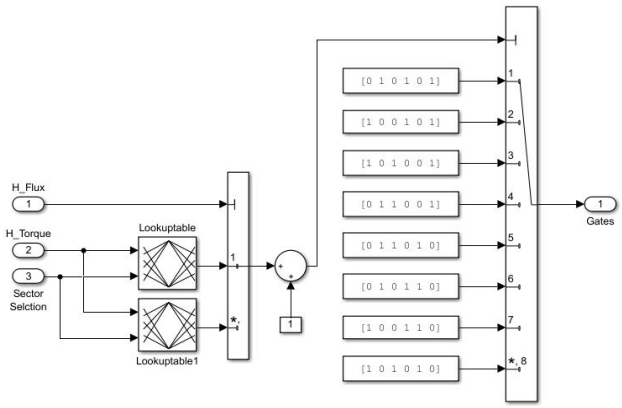

Fig. 14. Sub-block of Switching Table of the Inverter with DTC

Running the simulation for DTC scheme under the same condition as previous method. The electromagnetic varies in accordance with the load torque, therefor, the sawtooth shape has be eliminated by 75%, in result less noise occurred in comparison to 6-step scheme, furthermore, less variation in the Back-EMF waveform occurred in accordance with the load torque, as showing in Fig. 15 and Fig. 16, respectively,

The systematic variation of gate pulses results in nearly sinusoidal waveform of balanced 3-phase motor currents as showing in Fig. 17.

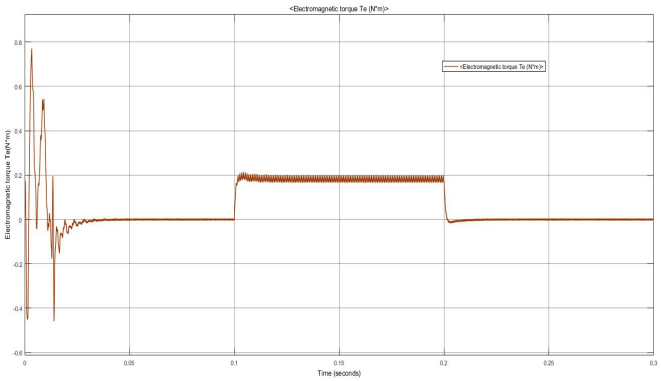

Fig. 15. Time vs Electromagnetic torque under load condition with DTC

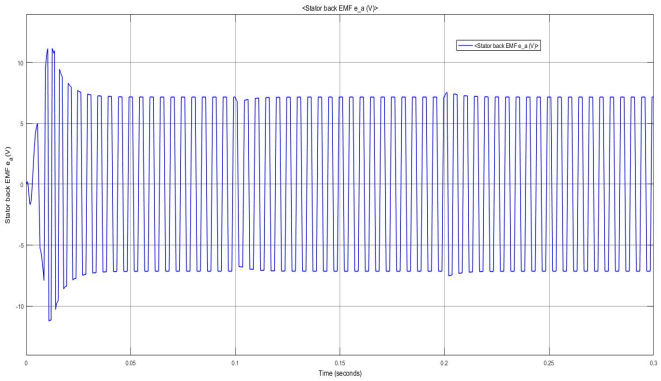

Fig. 16. Time vs Stator back-EMF under load condition with DTC

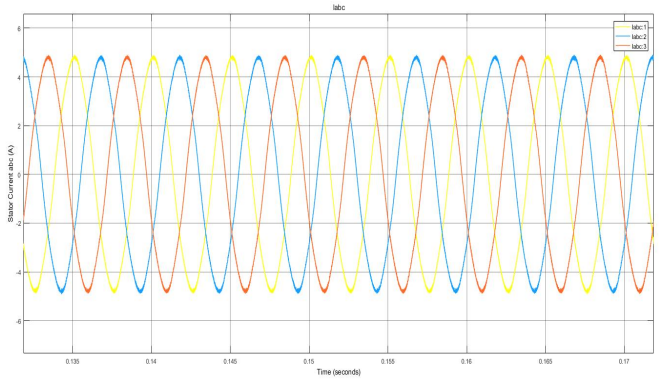

Fig. 17. Time vs Stator Current under load condition with DTC

The variation of actual and reference speed when load torque is applied at $t = 0.01s$ and removed at $t = 0.03s$, reference speed of $3000rpm$ is given to the system, under loaded condition, the performance characteristics of the system showing that the actual speed is following the reference speed from almost the starting point till the end of the simulation, also the undershooting and overshooting are minimized, cause the system being more stable achieves the required values with some steady state error, moreover, at the point we applied load the ripple have been minimized due to the fact that DTC improve the efficiency of the system, reduce noise and vibration of the motor in compare to other method, the time we removed the load, we see that the actual speed is getting

back to follow the reference speed as showing in Fig. 18 and Fig. 19, respectively.

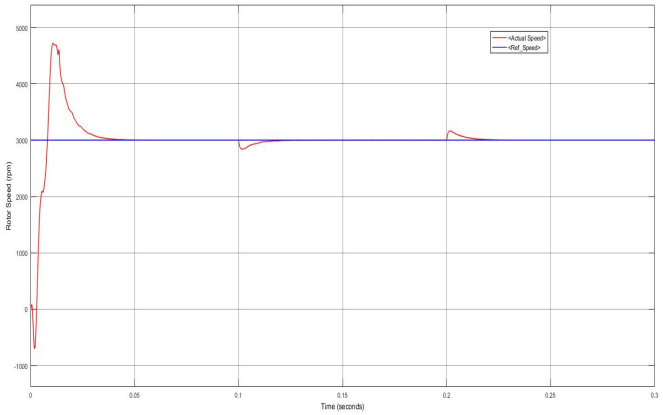

Fig. 18. Time vs Speed under load condition with DTC

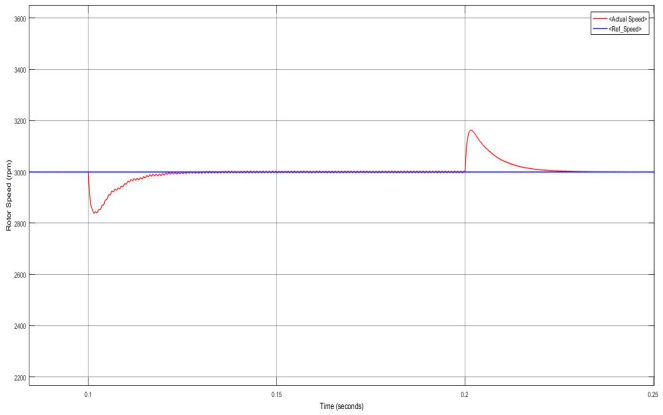

Fig. 19. Time vs Zooming Speed under load condition with DTC

Motor Parameters	
Back electromagnetic force	Trapezoidal
Number of poles paris, P	4
Rated Voltage (V)	24
Rated torque (Ncm)	20
Rated speed (rpm)	4400
Rated current (A)	5
Stator phase resistance Rs (ohm)	0.6
Stator phase inductance Ls (H)	0.6e-3
Rotor inertia (gcm^2)	52
Stator phase, star connection	3

TABLE II
BRUSHLESS DC MOTOR PARAMETERS

II. CONCLUSIONS

The performance of the six-step control and direct torque control scheme are investigated for the BLDC drive. The effectiveness of the proposed work is shown through in simulation using MATLAB/SIMULINK. The observed result showed that DTC based control results in fast torque response and improved performance of the system.

REFERENCES

[1] S. Ozcira, N. Bekiroglu and I. Senol, "Dynamic performance and analysis of direct torque control method based on DSP for PMSM drives," International Conference on Renewable Energy Research and Applications (ICRERA), Nagasaki, pp. 1-5, 2012.
[2] M. Masmoudi and B. E. Badsi and A. Masmoudi, "DTC of b4-inverter-fed BLDC motor drives with reduced torque ripple during sector-to-sector commutations," IEEE Transactions on Power Electronics, vol. 29, no. 9, pp. 4855-4865, 2014.
[3] H. Lu, L. Zhang, and W. Qu, "A new torque control method for torque ripple minimization of BLDC motors with un-ideal back EMF," IEEE Transactions on Power Electronics, vol. 23, no. 2, pp. 950958, Mar. 2008.
[4] M. A. Noroozi and J. S. Moghani and J. Mili Monfared and H. Givi, "An improved direct torque control of brushless DC motors using twelve voltage space vectors," 2012 3rd Power Electronics and Drive Systems Technology (PEDSTC), pp. 133-138, Feb. 2012.
[5] P. J. Sung, W. P. Han, L. H. Man, and F. Harashima, "A new approach for minimum-torque-ripple maximum-efficiency control of BLDC motor," IEEE Transactions on Power Electronics, vol. 47, no. 1, pp. 109114, Feb. 2000.
[6] Yong Liu , Z. Q. Zhu and David Howe, "Direct torque control of Brushless DC drives With reduced torque ripple," IEEE Transactions on Industry Applications, vol. 41, no. 2, pp. 559608, March. 2005.
[7] P.Devendra, Ch.Pavan Kalyan, K.Alice Mary, Ch.Saibabu, "Simulation Approach for Torque Ripple Minimization of BLDC Motor Using Direct Torque Control," International Journal of Advanced Research in Electrical, Electronics and Instrumentation Engineering, vol. 2, Issue 8, Aug. 2013.
[8] G. Kusuma, S.R Begum, N.N Teja, N.U Kumar, K. Satyanarayana, "Simulation of Brushless DC Motor using Direct Torque Control," Int. Journal of Engineering Research and Applications, Vol. 4, Issue 4 (Version 1), pp. 436-441, April 2014,

Hassan Hadeed received the B.Sc. in Information Systems degree from Ajman University of Science and Technology, Ajman, United Arab Emirates , in 2005. He is currently working toward M.Sc. of Engineering in Information Technology in the Department of Electrical Engineering and Information Technology at SRH University Heidelberg, Germany. His research interests include control of dynamic systems in particular electrical drives.

Achim Gottscheber received the Dipl.-Ing. (FH) degree from the Fachhochschule Aalen, Aalen, Germany, 1992 the M.Sc. degree from the University of London, King's College, London, UK, 1993 and the Ph.D. degree from the University of Mannheim, Mannheim, Germany. He is currently a Professor and Head of the department of Electrical Engineering and Information Technology at SRH University Heidelberg, Heidelberg, Germany. His research interests include controlled electrical drive systems, robotics, navigation and communication technology